Effects of Hemagglutinin Fusion Peptide on Poly(ethylene glycol)-Mediated Fusion of Phosphatidylcholine Vesicles†

Md. Emdadul Haque, Andrea J. McCoy, Julie Glenn, JinKeun Lee,‡ and Barry R. Lentz*

Department of Biochemistry and Program in Molecular/Cell Biophysics, University of North Carolina, Chapel Hill, North Carolina 27599-7260

Received June 22, 2001; Revised Manuscript Received September 7, 2001

ABSTRACT: The effects of hemagglutinin (HA) fusion peptide (X-31) on poly(ethylene glycol)- (PEG-) mediated vesicle fusion in three different vesicle systems have been compared: dioleoylphosphatidylcholine (DOPC) small unilamellar vesicles (SUV) and large unilamellar vesicles (LUV) and palmitoyloleoylphosphatidylcholine (POPC) large unilamellar perturbed vesicles (pert. LUV). POPC LUVs were asymmetrically perturbed by hydrolyzing 2.5% of the outer leaflet lipid with phospholipase A_2 and removing hydrolysis products with BSA. The mixing of vesicle contents showed that these perturbed vesicles fused in the presence of PEG as did DOPC SUV, but unperturbed LUV did not. Fusion peptide had different effects on the fusion of these different types of vesicles: fusion was not induced in the absence of PEG or in unperturbed DOPC LUV even in the presence of PEG. Fusion was enhanced in DOPC SUV at low peptide surface occupancy but hindered at high surface occupancy. Finally, fusion was hindered in proportion to peptide concentration in perturbed POPC LUV. Contents leakage assays demonstrated that the peptide enhanced leakage in all vesicles. The peptide enhanced lipid transfer between both fusogenic and nonfusogenic vesicles. Peptide binding was detected in terms of enhanced tryptophan fluorescence or through transfer of tryptophan excited-state energy to membrane-bound diphenylhexatriene (DPH). The peptide had a higher affinity for vesicles with packing defects (SUV and perturbed LUV). Quasi-elastic light scattering (QELS) indicated that the peptide caused vesicles to aggregate. We conclude that binding of the fusion peptide to vesicle membranes has a significant effect on membrane properties but does not induce fusion. Indeed, the fusion peptide inhibited fusion of perturbed LUV. It can, however, enhance fusion between highly curved membranes that normally fuse when brought into close contact by PEG.

Membrane fusion plays a vital and important role in many cellular processes. It is an essential step for entry of viruses into host cells. The detailed mechanism of PEG[1]-mediated cell membrane fusion is not known, nor is the mechanism by which fusion proteins induce cell membrane fusion. Influenza virus hemagglutinin- (HA-) mediated membrane fusion has been studied extensively. Influenza virus is endocytosed into target cells and releases its genome through fusion with the endosome membrane when the intravesicular pH drops to 5 (*1*, *2*). HA is produced as a single polypeptide chain that is stable at low pH (*3*). It is proteolytically cleaved at Arg^{329} to metastable HA monomers consisting of two subunits (HA1 and HA2) joined by a disulfide bridge. HA1 contains a binding site that recognizes and binds to the cell surface receptor, GM1. HA2 is the fusion machine. A highly conserved 20-amino acid segment of residues at the N-terminus of HA2 is essential for fusion activity (*4*) and this hydrophobic segment is called a "fusion peptide". HA monomers are organized into a trimer that undergoes a conformational change at the low pH of the endosome (*5*). It has been proposed that free energy released during this conformational change allows work to be done on the lipid bilayer in a way that catalyzes the fusion process (*6*).

The necessary condition for membrane fusion between two adjacent bilayers is the formation of a small fusion pore, which is created through the reorganization of lipid bilayers at their contact region (*7*). The fusion peptide inserts into the target membrane early in the fusion process and also inserts into the viral membrane at some point during the process (*8*). This has led to many studies of fusion peptide interactions with model membrane vesicles (*9*). Many articles have been published to document aggregation and fusion of model membranes induced by these peptides or specific amino acid mutants of these peptides (*10*−*15*). Unfortunately, most of these studies have used peptide/lipid ratios above 1/50, have followed only membrane connectivity as a measure of fusion, or have used assays that confuse leakage of contents with mixing of contents. Despite the clear

† Supported by USPHS Grant GM 32707 to B.R.L.

* To whom correspondence should be addressed: e-mail uncbrl@med.unc.edu.

‡ Present address: Transave company, 7 Deer Park Dr., Monmouth Park, NJ 08850.

[1] Abbreviations: DOPC, 1,2-dioleoyl-3-*sn*-phosphatidylcholine; POPC, 1-palmitoyl-2-oleoyl-3-*sn*-phosphatidylcholine; LPC, lysophosphocholine; DPH, 1,6-diphenyl-1,3,5-hexatriene; DPH_pPC, 1-hexadecanoyl-2-(3-(diphenylhexatrienyl)propanoyl)-*sn*-glycero-3-phosphocholine; SUV, small, unilamellar vesicles made by the sonication technique; LUV, large unilamellar vesicles made by the extrusion technique; PEG, poly(ethylene glycol); PLA_2, phospholipase A_2; BSA, bovine serum albumin; QELS, quasi-elastic light scattering; ANTS, 8-aminonaphthalene-1,3,6-trisulfonic acid; DPX, *N*,*N*′-*p*-xylylenebis(pyridinium bromide); HPTS, 8-hydroxypyrene-1,3,6-trisulfonic acid; $C_{12}E_8$, octaethylene glycol mono-*n*-dodecyl ether; TES, *N*-[tris(hydroxymethyl)-methyl]-2-aminoethanesulfonic acid.

10.1021/bi011308l CCC: $20.00 © 2001 American Chemical Society
Published on Web 11/02/2001

evidence of the importance of the N-terminal fusion peptide of the HA2 subunit to viral fusion, there is no clear indication as to whether this 20 amino acid residue peptide induces fusion of pure lipid bilayers.

In the present study, our goals were (i) to determine whether the HA fusion peptide can induce membrane fusion even at high concentrations, (ii) to determine the nature of the lipid bilayers that the HA fusion peptide can induce to fuse, and (iii) to define the affinity of peptide to the different lipid bilayer surfaces. To reach these goals, we have focused on the effect of HA fusion peptide from X31 strain (X-31) on poly(ethylene glycol)- (PEG-) mediated vesicle fusion in three different systems: sonicated vesicles (SUVs), extruded unilamellar vesicles (LUVs), and perturbed LUVs. PEG has two effects on vesicles that help promote fusion. First, it aggregates vesicles without interacting directly with them (*16*), and second, it provides a compressive osmotic stress that makes vesicles more fusogenic (Malinin and Lentz, unpublished observations). Fusion peptides are well-known to aggregate liposomes, but they do so at concentrations where they are reported to induce liposome rupture. Our purpose in studying these two agents together was to examine the effect of peptide on the fusion of aggregated vesicles at peptide concentrations low enough that the peptide should not induce vesicle rupture. Our results show that the HA fusion peptide does not induce membranes to fuse but can enhance PEG-mediated fusion between already fusogenic vesicles.

EXPERIMENTAL PROCEDURES

Materials

Chloroform stocks of 1,2-dioleoyl-*sn*-glycero-3-phosphatidylcholine (DOPC) and 1-palmitoyl-2-oleoyl-*sn*-glycero-3-phosphatidylcholine (POPC) were purchased from Avanti Polar Lipids, Inc. (Birmingham, AL) and used without further purification. Phospholipase A_2 (PLA_2) purified from the venom of *Agkistrodon piscivorus piscivorus* was kindly provided by Professor R. Biltonen of University of Virginia (Charlottesville, VA). The sodium salt of 8-aminonaphthalene-1,3,6-trisulfonic acid (ANTS), *N*,*N*′-*p*-xylylenebis-(pyridinium bromide) (DPX), 1-hexadecanoyl-2-(3-(diphenylhexatrienyl)propanoyl)-*sn*-glycero-3-phosphocholine (β-DPHpPC), and the trisodium salt of 8-hydroxypyrene-1,3,6-trisulfonic acid (HPTS) were purchased from Molecular Probes (Eugene, OR). *N*-[Tris(hydroxymethyl)methyl]-2-aminoethanesulfonic acid (TES) and bovine serum albumin (BSA) were purchased from Sigma Chemical Co. (St. Louis, MO). Dodecyl octaethylene glycol monoether ($C_{12}E_8$) was purchased from Calbiochem (La Jolla, CA). Poly(ethylene glycol) of molecular weight 7000−9000 (PEG) was purchased from Fisher Scientific (Fairlawn, NJ) and purified as described previously (*18*). Polybead polystyrene microspheres were purchased from Polysciences, Inc. (Warrington, PA). All other reagents were of the best quality available.

Methods

Vesicle Preparation. Large unilamellar vesicles (LUVs) were prepared by the extrusion method (*17*). Lipid suspensions were extruded seven times through a 0.1 μm polycarbonate filter (Nucleopore Corp., Pleasanton, CA) at room temperature (above the phase transition) under a pressure of 100 psi of nitrogen (*18*). Small unilamellar vesicles (SUVs) were prepared by sonication and fractionated as previously described (*19*). Chloroform stocks of DOPC or POPC with or without appropriate amounts of fluorescence probe (DPH_P-PC) were mixed and dried under a stream of nitrogen. The dried lipids were dissolved in cyclohexane and methanol (about 5 vol %), frozen on dry ice, and dried overnight under high vacuum. The dried lipids were suspended in appropriate buffers and agitated for 20−40 min at room temperature. For SUV preparation, the lipid suspension was sonicated for 10−15 min at 4 °C by a Heat System model 350 sonicator (Plainview, NY) equipped with a titanium probe tip of 9.5 mm diameter. Vesicles were fractionated by centrifugation at 70 000 rpm for 25 min at 4 °C in a Beckman TL-100 ultracentrifuge (Palo, Alto, CA). For the ANTS/DPX contents mixing assay, lipids were suspended in buffer containing 10 mM TES, 25 mM ANTS (or 90 mM DPX), and 40 mM NaCl (pH 5.0). For the ANTS/DPX content leakage assay, lipids were suspended in buffer containing 10 mM TES, 12.5 mM ANTS, 45 mM DPX, and 40 mM NaCl (pH 5.0). Untrapped buffer was removed from the vesicles by use of a Sephadex G-75 column equilibrated with 2 mM TES, 100 mM NaCl, and 1 mM EDTA, pH 5.0 (DOPC vesicles) or 2 mM TES and 100 mM NaCl, pH 7.4 (buffer for POPC vesicles). For the assays of PLA_2 activity with HPTS, lipids were suspended in buffer containing 100 mM NaCl (pH 7.4). For peptide binding experiments, vesicles were suspended in 2 mM TES, 100 mM NaCl, and 1 mM EDTA buffer, pH 5.0.

Preparation of Perturbed Outer Leaflet Vesicles. A protocol involving limited PLA_2 hydrolysis was adapted from Burack et al. (*20*) and modified as described (*21*). POPC LUVs (10 mM) in pH 7.4 buffer were incubated with 2 mM $CaCl_2$ and 10 μM PLA_2 at 10 °C for 1 h. The hydrolysis reaction was stopped by addition of 4 mM EDTA, and vesicles were incubated on ice with 0.5 mM BSA (*22*, *23*) for 20 min to remove the hydrolysis products, lyso-PC (LPC) and oleoylate, from the membrane outer leaflet. Hydrolysis products bound to BSA as well as enzyme were separated from the LUV by use of a Sepharose CL-4B column equilibrated with 2 mM TES, 100 mM NaCl, and 1 mM EDTA buffer, pH 5.0, at 2−4 °C. Fluorescence measurements and fusion assays were performed within 2 h of BSA treatment.

The amount of hydrolysis was determined by an assay involving the fluorescent dye HPTS, whose fluorescence is quenched by protonation. A standard curve was established for LUV (10 mM, pH 7.4) with 2 mM $CaCl_2$ (pH 7.4), 100 μM HPTS (pH 8.0), and 100 mM NaCl (pH 7.4) solution at 10 °C. HCl was titrated into the solution, and the fluorescence intensity change with respect to the pH change was determined. The fluorescence intensity change of another sample of 10 mM LUV, 2 mM $CaCl_2$, 100 μM HPTS, and 100 mM NaCl, pH 7.4, was monitored at 10 °C for 30−60 min after the addition of 10 μM PLA_2. A control experimental sample without LUV was also monitored to determine the pH change due to CO_2 dissolution in the sample. The intensities were normalized to the initial fluorescence intensity of the standard curve, the control was subtracted from the experimental curve, and the fluorescence intensity was used to obtain the

concentration of hydrolysis product in terms of the concentration of protons released. Because the enzyme activity was sensitive to pH, the experiment was performed at an initial pH of 7.4, and the initial slope of the curve was calculated and taken as the enzyme activity (micromoles of H^+ per second). The amount of hydrolysis was calculated to be 2.5% of the overall lipid concentration (5% of the outer leaflet) after 1 h of incubation of vesicles in a pH 7.4 buffer.

Preparation of HA Peptide. The X-31 HA fusion peptide (GLFGAIAGFIENGWEG MIDG) was chemically synthesized and purified by The Protein Chemistry Lab of UNC-CH using t-Boc procedures. The peptide was synthesized by solid-phase synthesis at the C-terminal carboxamides on an Applied Biosystems 430 peptide synthesizer (Perkin-Elmer Applied Biosystems, Foster City, CA) with *t*-Boc protected amino acids and Bha resin (Perkin-Elmer Applied Biosystems, Foster City, CA). Coupling times were 40 min. The peptide was cleaved by two different cleavage methods: low and high cleavage. The low cleavage of the peptide involved treatment with ethanedithiol/trifluoroacetic acid/dimethyl sulfoxide/trifluoromethanesulfonic acid/*m*-cresol (200:5:4:1:0.8) for 2 h at −5 to 0 °C and precipitation by the addition of ether. The peptide was then subjected twice to the high cleavage, which involved treatment with hydrofluoric acid/anisole/dimethyl sulfoxide (10:1:1) for 2 h at −5 to 0 °C and precipitation by the addition of ether. The precipitated peptide was extracted after one wash with water, four washes with ammonium acetate, and two more washes with water. After neutralization of the extract, the sample was frozen and lyophilized for 48 h. The peptide was then dissolved in guanidine/Tris and purified on a Rainin HPLC (Rainin, Emeryville, CA) and a 22 × 250 Vydac 214TP (Vydac, Hesperia, CA) column at a flow rate of 25 mL/min. The major peak was lyophilized and stored at −20 °C. Amino acid determination confirmed the peptide identity, and mass spectroscopy showed the dried product to be more than 90 wt % of the proper peptide. Because X-31 peptide associates well with LUV at pH 5.0 (*13*), all experiments involving the X-31 peptide were performed at pH 5.0. For binding experiments, the peptide was dissolved in DMSO, and small aliquots of this solution were added to vesicle samples. DMSO was always less than 1% of the buffer volume at the completion of the titrations, and control experiments showed that this amount of DMSO had no effect on the surface properties or fusion ability of vesicles used in this study. For all other experiments, the peptide was dissolved in 2 mM TES and 100 mM NaCl buffer, pH 7.4, with gentle rocking.

ANTS/DPX Contents Mixing and Leakage Measurements. The ANTS/DPX contents mixing and leakage assays have been described previously (*24*) and modified for PEG-mediated fusion (*18*). To determine contents mixing at different PEG concentrations, ANTS-containing vesicles (0.25 mM) and DPX-containing vesicles (0.25 mM) in equal amounts were incubated with PEG in a 0.4 mL volume before dilution to a final volume of 3.5 mL. For the contents leakage assays, vesicles coencapsulating both ANTS and DPX (0.5 mM) were incubated in PEG in a 0.4 mL volume before dilution to a final volume of 3.5 mL. For the contents mixing and leakage assays at different peptide concentrations, vesicles similar to those above were mixed with peptide before incubation in a 20 wt % PEG solution (final volume of 0.4 mL) for 3 min at room temperature before dilution to a final volume of 3.5 mL. Fluorescence measurements were taken on the fourth minute and analyzed to give the amount of contents mixing and leakage as described previously (*18*). For contents mixing, the fluorescence intensity of ANTS-containing vesicles (with peptide when applicable) in PEG was taken to be representative of 0% contents mixing. The calculation of "percentage contents mixing" was based on the assumption (*18*) of one "ideal round" of fusion, i.e., fusion occurring between pairs of aggregated vesicles. Therefore, the fluorescence intensity of coencapsulated ANTS/DPX vesicles (with peptide when applicable) plus PEG characterized 100% contents mixing. The calculated content mixing values will thus be underestimated as noted previously (*25*). The contents mixing calculations also accounted for the probability that two fusing vesicles contained ANTS or DPX, for the leakage of contents, and for the photobleaching of ANTS (*18*). The fluorescence intensity of the coencapsulated vesicles (with peptide when applicable) plus the background intensity contributed by PEG represented 0% leakage. Correspondingly, 100% leakage was characterized by the fluorescence intensity of an ANTS/DPX vesicle sample (with peptide when applicable) in which the vesicle contents were released by the addition of detergent ($C_{12}E_8$ at 0.46 mM final concentration), plus a PEG background.

Lipid Mixing Measurements. The transfer of lipids between contacting membranes of SUVs and LUVs was detected by a change in the fluorescence lifetime of DPH_PPC (*26*). This fluorescent lipid shows a much smaller fluorescent lifetime when incorporated into vesicles at high surface concentration than it reports at dilute surface concentrations (*27*). Thus, this assay reports transfer of DPH_PPC from probe-containing to probe-free vesicles as an increase in average lifetime. All fluorescence measurements were made on an SLM 48000 MHF spectrofluorometer (SLM Instruments, Rochester, NY) equipped with a Coherent Inova 90 argon-ion laser (Coherent Auburn Group, Auburn, CA) by use of the laser UV multiline (351.1−363.8 nm) for DPHpPC. Emission was detected at an angle of 54.7° from the vertical through a 3 mm KV-450 filter (Schott Optical Glass, Duryea, PA). Phase shifts and modulation ratios at 30 frequencies (with a base frequency of 4 MHz) with a 5 s acquisition time, 300-acquisition average, and a glycogen solution as zero lifetime were collected by acquisition software of the SLM 48000.

The lifetimes of DPHpPC in SUVs, LUVs, and perturbed LUVs with different lipid:probe ratios (final lipid concentration of 0.5 mM) plus peptide in 20 wt % PEG were obtained at 23 °C and a standard curve was determined for each vesicle system. These calibration curves were used to translate DPH_PPC lifetime into percent lipid mixing. A mixture of probe-free and probe-rich vesicles (10:1) was mixed with appropriate concentrations of peptide and PEG, and lifetime data were collected. The data were analyzed with the assumption of three lifetime components for each peptide or PEG addition. The phase-resolved lifetimes and intensity fractions of each component were calculated with the Global Analysis software package (Globals Unlimited, Urbana, IL) and the average lifetime under each set of conditions was thereby determined.

Peptide Binding. Binding was detected either by an increase in tryptophan fluorescence when vesicles were added

to peptide or by energy transfer from tryptophan to membrane-associated DPH when peptide was added to vesicles. For detection of enhanced tryptophan fluorescence, increasing amounts of SUV (or LUV) were added to 2 μM peptide, and the emission spectra were recorded from 290 to 400 nm. A control emission spectrum was also obtained by addition of increasing amounts of SUVs (or LUVs) to a solution containing no peptide, and this spectrum was subtracted from the spectrum with peptide. For the determination of energy transfer from the excited state of tryptophan to the membrane-bound DPH, increasing amounts of peptide were added to 500 μM SUVs (or LUVs) containing DPH (250:1 lipid: probe) and to 500 μM SUVs (or LUVs) without DPH. Tryptophan was excited at 280 nm and the emission spectra were obtained from 295 to 540 nm by use of a monochromator, with slit widths of 4/4 for the excitation and emission light, and no filter. The control spectrum (no probe) was subtracted from the spectrum in the presence of probe to obtain the fluorescence intensity change at λ_{max}. Global analysis of the data to obtain binding parameters was carried out with the program SCOP (Simulation Resources, Berrien Spring, MI) as described previously (*28*).

Determination of Vesicle Diameters. Changes in average particle diameter in mixtures of vesicles with peptide were determined by quasi-elastic light scattering measurements (QELS). QELS measurements were performed on a locally built multiangle instrument equipped with a Spectra-Physics Stabilite Model 120S helium−neon laser (632.8 nm) and a computer-controlled Nicomp 170 autocorrelator (Particle Sizing Systems, Inc., Santa Barbara, CA) (*18*). Peptide at a series of concentrations was added to vesicle samples (500 μM SUV or 200 μM LUV, pH 5.0), and size determinations were performed after 15 min by comparison to polystyrene microspheres of known size. Autocorrelation functions were analyzed either by assuming a single Gaussian distribution of particle sizes or by assuming a sum of Gaussian peaks with software provided by Particle Sizing Systems.

RESULTS

Binding of HA Fusion Peptide (X-31) to DOPC and POPC Vesicles. Figure 1 shows the binding of X-31 HA fusion peptide (2 μM) to DOPC SUV and LUV and POPC perturbed LUV as monitored by measuring the change in tryptophan fluorescence intensity with the addition of increasing concentration of the lipid vesicles. A saturable increase in tryptophan fluorescence was observed in all cases. The intensity change at saturation was larger for SUVs than for LUVs as we expected.

Binding of X-31 to DOPC SUVs, LUVs, and POPC perturbed LUVs was also monitored by fluorescence resonance energy transfer from the excited state of tryptophan to membrane-bound DPH. Tryptophan and DPH form an efficient fluorescence donor−acceptor pair. Figure 2 shows the increase in fluorescence intensity of membrane-bound DPH as a result of energy transfer from increasing concentrations of peptide. In all three cases, a clear saturation was observed at high concentration of peptide. Binding parameters were obtained by fitting both sets of data as described previously (*28*) with the resulting, best-fit parameters summarized in Table 1. The K_ds increased in the order DOPC SUVs < perturbed POPC LUVs < DOPC LUVs, meaning

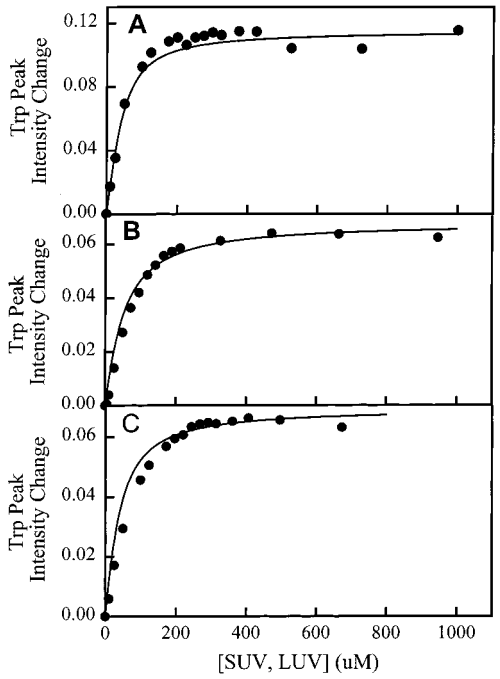

FIGURE 1: HA fusion peptide binding to different membrane surfaces judged by Trp intensity change. Peptide binding to (A) DOPC SUVs, (B) DOPC LUVs, and (C) perturbed POPC LUVs was detected by Trp fluorescence intensity increase as a function of lipid concentration (micromolar) at 23 °C. Measurements were carried out with 2 μM peptide in 2 mM TES, 100 mM NaCl, and 1 mM EDTA buffer, pH 5.0. The lines drawn through the data show the result of fitting these and the data in Figure 2 globally to a simple membrane-binding model (*28*).

that the peptide bound more tightly to membranes that had a perturbed surface.

K_d values have been reported for the same peptide binding to POPC LUV [0.5 to 0.8 μM (*13*)] and SUV [0.17 μM for SUVs (*11*)], with stoichiometries (*i*) of 50 and 40 lipids per protein bound at saturation, respectively. While our values disagree with these literature values, the products $K_d i$ agree fairly well between our values and reported values. This is because these binding parameters are linked and it is difficult to obtain both from a single experiment. We have estimated these parameters by globally fitting two data sets, a procedure that should allow better estimates of binding stoichiometries than one can obtain from a single experiment, and this may explain the difference between our values and those in the literature.

Aggregation of Vesicles by HA Fusion Peptide. We have evaluated by QELS the ability of the HA fusion peptide to aggregate vesicles in the absence of PEG. The aggregation of DOPC SUVs and LUVs and POPC perturbed LUV by X-31 fusion peptide was monitored by measuring the change in vesicle diameter as determined by QELS, with data analyzed by two models, one assuming a single Gaussian distribution of particle sizes and the second allowing for multiple Gaussian distributions. The results are represented in Figure 3 as a function of peptide/lipid ratio. When QELS data were analyzed in terms of a single Gaussian, DOPC SUV were estimated to be roughly 20 nm in diameter in the absence of peptide, but increased in size even at very low peptide/lipid ratio (● in Figure 3). However, additional information was obtained when QELS data were analyzed in terms of multiple Gaussian distributions. One population

Table 1: Effects of Fusion Peptides on Different Membranes

	DOPC SUV	DOPC LUV	pert. POPC LUV
K_d (μM)	0.96	2.86	1.26
stoichiometry[a]	13	6	7.5
effect on fusion	enhances, then inhibits	no fusion	inhibits
effect on leakage	enhances	enhances	enhances
effect on lipid mixing	enhances	enhances	inhibits
aggregation	promotes	none, then promotes	none, then promotes

[a] Outer leaflet lipid/peptide ratio is shown.

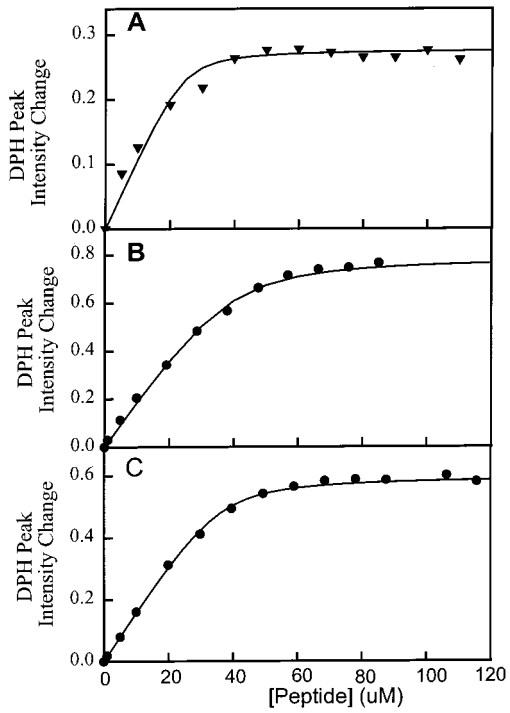

FIGURE 2: HA fusion peptide binding to different membrane surfaces as judged by Trp-to-DPH energy transfer. Peptide binding to (A) DOPC SUVs, (B) DOPC LUVs, and (C) perturbed POPC LUVs was followed by DPH fluorescence increase due to Trp to DPH energy transfer as a function of peptide concentration. Measurements were carried out on 500 μM lipid vesicles containing DPH at a lipid-to-probe ratio of 250:1. The buffer composition, pH, and temperature were the same as in Figure 1. The lines drawn through the data show the result of fitting these and the data in Figure 1 globally to a simple membrane-binding model (*28*).

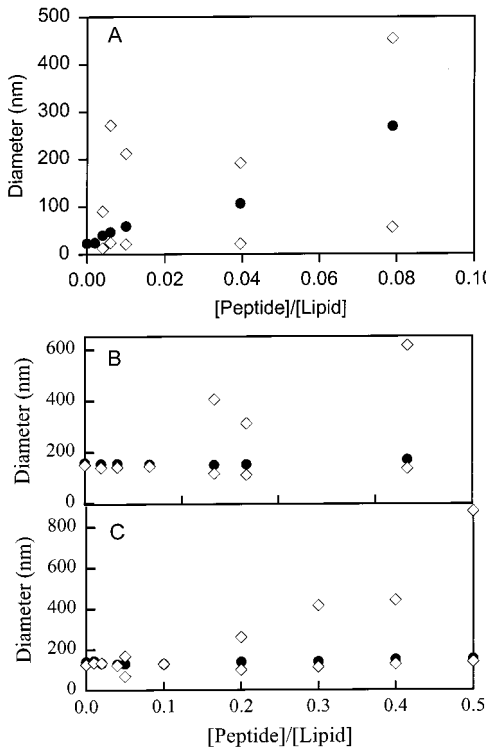

FIGURE 3: Effect of HA fusion peptide on vesicle size. Diameters of vesicles, as determined by QELS, are plotted as a function of P/L ratio. Peptide was added at increasing concentrations to (A) DOPC SUVs, (B) DOPC LUVs, and (C) perturbed POPC LUVs and their size was estimated from a single Gaussian distribution (●) or by a multiple Gaussians method (◇) to estimate diameters from measured autocorrelation functions. The total lipid concentration was 500 μM for SUV and 200 μM for LUV. Measurements were carried out in 2 mM TES, 100 mM NaCl, and 1 mM EDTA at pH 5.0.

was detected in untreated DOPC SUV, i.e., these were monodisperse. When peptide was added up to a P/L of about 0.01, this 20 nm population remained, but a second, considerably larger population was found to increase in size and contribution with increasing P/L ratio (◇ in Figure 3). DOPC LUVs and POPC perturbed LUVs remained monodisperse and maintained a constant particle size even up to high peptide concentration (Figure 3B,C). We found, however, that DOPC LUV and perturbed POPC LUVs also became polydisperse (i.e., were best described by two populations of particle sizes) at high concentrations of peptide, one that remained constant and one that increased with P/L ratio (◇ in Figure 3B,C). These results clearly demonstrate that the HA fusion peptide was able to aggregate highly curved and uncurved DOPC and perturbed POPC vesicles at pH 5 but that much higher concentrations of peptide were needed to aggregate uncurved LUVs than highly curved SUVs.

Effect of HA Fusion Peptide on Contents Mixing (Fusion), Leakage, and Lipid Mixing of DOPC SUV in the Absence of PEG. The extents of leakage (A, ●) and contents mixing (A, ▲) in DOPC SUV are plotted in Figure 4 as a function of peptide/lipid ratio. At low P/L ratio (less than 0.01), a small amount of leakage and lipid mixing was observed. However, above this P/L ratio, leakage increased in direct proportion to increasing peptide/lipid ratio without any accompanying contents mixing. Lipid transfer between vesicles increased in an S-shaped fashion with increasing surface occupancy (Figure 4B, ●). At high P/L, this mimicked the variation of surface occupancy with P/L ratio (Figure 4B, solid line) but clearly did not show a hyperbolic behavior at low P/L. Contents mixing with minimal leakage is necessary and sufficient to indicate fusion. The fact that this condition was not met clearly demonstrates that HA fusion peptide is unable to induce fusion even at very high surface occupancy at pH 5. It was, however, able to aggregate

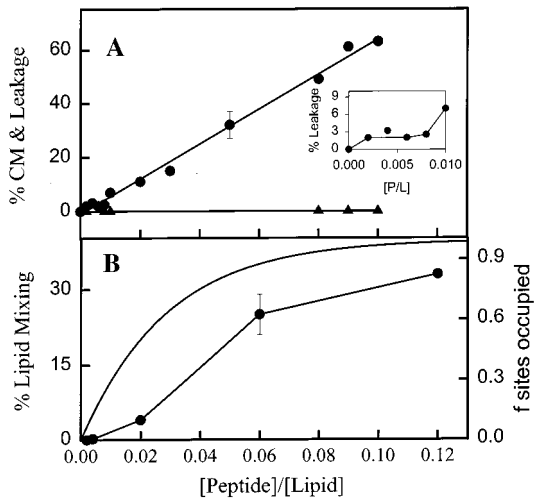

FIGURE 4: Effect of HA fusion peptide on DOPC SUVs in the absence of PEG. (A) Vesicle contents mixing and contents leakage and (B) lipid mixing for DOPC SUVs are shown as a function of peptide/lipid ratio. Contents mixing and leakage experiments were carried out with 500 μM DOPC SUVs in 2 mM TES, 100 mM NaCl, and 1 mM EDTA, pH 5.0. Lipid mixing experiments were carried out with 500 μM DOPC SUVs and 50 μM DPHpPC/DOPC (1:10) SUVs in 2 mM TES, 100 mM NaCl, and 1 mM EDTA, pH 5.0. The inset to panel A shows in more detail the variation of leakage data at low peptide/lipid ratio. Most experiments were done twice, with representative standard error bars shown for experiments performed 3−4 times. The fraction of membrane surface sites occupied was calculated from the binding parameters recorded in Table 1 to obtain the hyperbolic plot shown as a solid line.

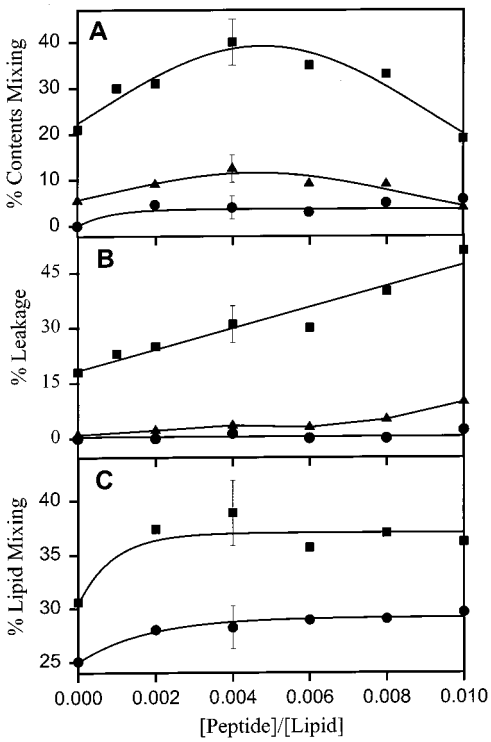

FIGURE 5: Effect of HA fusion peptide on DOPC SUVs aggregated by PEG. Vesicle contents mixing (A), contents leakage (B), and lipid mixing (C) are plotted as a function of peptide/lipid ratio in the presence of different PEG concentrations: 10 wt % PEG (●); 15 wt % PEG (▲); and 20 wt % PEG (■). Experimental conditions and assays are the same as for Figure 4. Representative error bars are shown.

vesicles, induce lipid mixing, and destabilize DOPC SUV at higher P/L ratios.

Effect of HA Fusion Peptide on Highly Curved DOPC SUVs in the Presence of PEG. Figure 5 shows the influence of HA peptide on contents mixing (A), contents leakage (B), and lipid mixing (C) of DOPC SUV as a function of peptide/lipid ratio when vesicles are aggregated by 10 (●), 15 (▲), and 20 (■) wt % PEG. At 10 wt % PEG, DOPC SUVs did not fuse but they did aggregate and their outer leaflets mixed. Contents mixing increased slightly up to about a P/L ratio of 0.004 at 10 wt % PEG (Figure 5A) without any significant accompanying leakage (Figure 5B). The peptide also enhanced lipid transfer up to a P/L ratio of 0.002 (Figure 5C). At 15 and 20 wt % PEG, contents mixing was enhanced in DOPC SUV at low surface occupancy and hindered at high surface occupancy, while leakage gradually increased with increasing P/L ratio (Figure 5A,B). We conclude from these results that the HA fusion peptide enhanced fusion of fusogenic vesicles aggregated by PEG without inducing significant leakage at low percentages of PEG (10 and 15 wt %). These results also indicate that the peptide enhanced fusion of these highly curved, fusogenic vesicles at low surface occupancy (peptide/lipid ratio ~0.004) but inhibited fusion at higher surface occupancies at higher PEG concentrations. One could argue that the inhibition seen at higher P/L ratios is due to increased leakage. However, we routinely correct contents mixing data for contents leakage, and in our experience, we can measure contents mixing reliably in the presence of even 50−60% contents leakage. In addition, to be sure that leakage was not the reason for this peptide-induced inhibition of PEG-mediated fusion, we carried out an experiment at 15% PEG, under which conditions leakage was essentially zero (Figure 5B, ▲). Although contents mixing was much less dramatic at 15% PEG, the trend with increasing peptide concentration was just as we found at 20% PEG. Peptide also enhanced lipid mixing between highly curved vesicles, but this effect maximized at very low surface occupancy and remained constant at higher peptide concentrations (Figure 5C).

Effect of HA Fusion Peptide on Fusion of Uncurved DOPC Vesicles. PEG-induced leakage and contents mixing (panel A) and lipid mixing (panel B) of DOPC LUVs are recorded in Figure 6 as a function of peptide/lipid ratio at a fixed PEG concentration (20%). As we have previously reported (*29*), DOPC (LUVs) vesicles do not fuse at any PEG concentration, even though substantial lipid exchange occurs, and a good fraction of their contents is lost. In the present study, the extent of leakage increased substantially with added peptide, while lipid mixing increased gradually without any contents mixing being observed at any P/L ratio. These results show that LUVs behave differently with respect to HA fusion peptide from highly curved vesicles (SUVs). As for SUV, HA fusion peptide can destabilize the membranes bilayer, leading to significant amount of leakage or rupture but not to fusion.

Effect of Peptide on PEG-Induced Fusion of Perturbed POPC LUVs. The extents of PEG-mediated leakage and contents mixing (panel A) and lipid mixing (panel B) of perturbed POPC LUVs are shown in Figure 7 as a function of PEG concentration. The extent of lipid mixing was very low up to 10 wt % PEG, while substantial lipid transfer occurred above 15 wt % PEG (Figure 7B). A substantial amount of contents mixing was observed at 20 wt % PEG without any significant accompanying leakage. This confirms

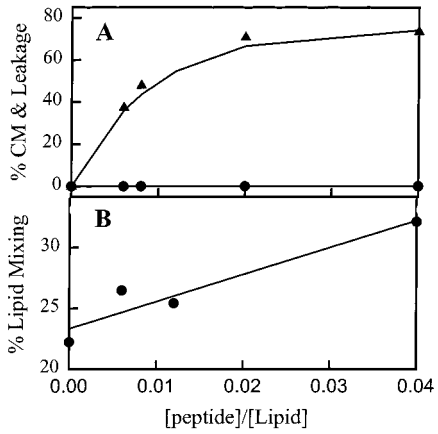

FIGURE 6: Influence of fusion peptide on DOPC LUVs in the presence of PEG. (A) Vesicle contents leakage (▲) and contents mixing (●) and (B) lipid mixing (●) for DOPC LUVs are plotted as a function of peptide/lipid ratio at a fixed PEG concentration (20 wt %). Experimental conditions and assays are the same as for Figure 4.

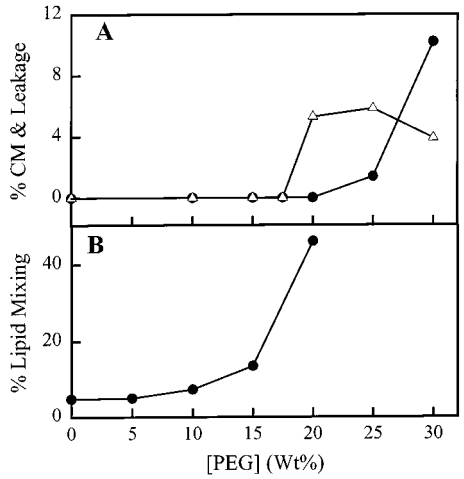

FIGURE 7: PEG profile of perturbed POPC LUVs. (A) Vesicle contents leakage (●) and contents mixing (△) and (B) lipid mixing of pert. POPC LUVs (●) are shown as a function of PEG concentration. Experimental conditions and assays are the same as for Figure 4.

our previous observation that leakage is not inherently a part of the fusion process (*30, 31*).

Because HA fusion peptide enhanced fusion of highly curved SUVs that have a perturbed outer leaflet, we have also tested the effect of HA fusion peptide on PEG-mediated (20 wt %) fusion of pert. LUV. Figure 8A,B shows that contents mixing of perturbed LUVs decreased and leakage increased with increasing peptide concentration. These results clearly indicate that the HA fusion peptide inhibited fusion and enhanced leakage in outer leaflet-perturbed POPC LUVs. Figure 8 presents the extent of lipid mixing in the presence (panel C) and absence (panel D) of PEG as a function of P/L ratio. The extent of lipid transfer in the absence of PEG remained unchanged with increasing P/L ratio; peptide hindered lipid mixing in the presence of PEG but only for the perturbed vesicles. These results suggest that the HA fusion peptide fills the packing defects in perturbed LUV and inhibits the initial step leading to fusion (*21*). This is consistent with the report that HA fusion peptide induces negative curvature strain (*32*). Addition of agents with negative intrinsic curvature (e.g., lysophosphatidylcholine)

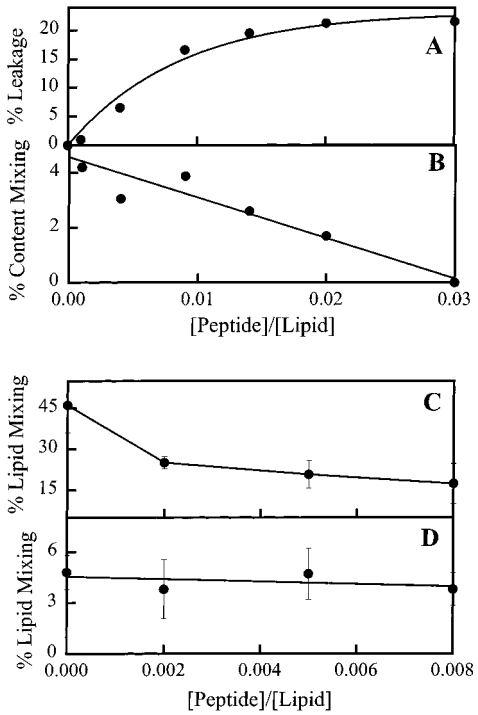

FIGURE 8: Effect of HA fusion peptide on perturbed POPC LUVs aggregated by PEG. Leakage (A) and contents mixing (B) of perturbed POPC LUVs are plotted as a function of peptide/lipid ratio in the presence of 20 wt % PEG. Lipid mixing between vesicles aggregated by (C) or untreated with 20 wt % PEG (D) are plotted as a function of peptide/lipid ratio. Measurements were carried out as described in Figure 4.

to contacting vesicle leaflets is generally recognized as inhibiting the initial step (contacting-leaflet merging) of the fusion process (*33*).

DISCUSSION

HA-mediated cell as well as model membrane fusion is well studied (*34*−*46*). Protein machines act on lipid bilayers to bring membranes close together and then somehow to encourage fusion pore formation. Even though a vast literature is available on HA-mediated membrane fusion, it is still not clear how HA catalyzes fusion, and it is not really known whether fusion peptide plays an active role to induce membrane fusion. With the intent of asking whether HA fusion peptide might influence fusion in a well-defined model system, we have documented in the present studies the effect of HA fusion peptide on fusion of model membranes with different curvatures and surface properties in the presence and absence of PEG.

We have reached the following conclusions:

(1) Fusion peptide at high P/L ratio aggregates vesicles, causes intervesicle lipid transfer, and ruptures vesicles but does not induce fusion.

(2) Fusion peptide enhances PEG-mediated fusion only of highly curved, fusogenic vesicles at low P/L ratios but inhibits fusion at high P/L.

(3) Fusion peptide affects both the initial and subsequent steps of the fusion process, and it is unclear from the present study which is most affected.

(1) **Fusion peptide at high P/L ratio aggregates and ruptures vesicles, causes intervesicle lipid transfer, and ruptures vesicles but does not induce fusion**. In the absence

of PEG, the HA peptide had a minor effect on membrane destabilization (evidenced by low leakage) and outer leaflet mixing of DOPC SUVs (Figure 4) up to a P/L ratio of 1:50. A significant amount of lipid transfer and leakage was observed at high peptide/lipid ratio without any accompanying contents mixing (Figure 4). The fusion peptide destabilized the bilayer of DOPC SUVs and made these vesicles leaky instead of inducing fusion. The several reports in the literature purporting to show HA peptide-induced fusion (*10*−*14*) actually were seeing aggregation of vesicles, outer leaflet mixing, or rupture instead of fusion at high peptide concentration.

The effect of fusion peptide is different in the presence of sufficient PEG to induce fusion of fusogenic vesicles. (2) **Fusion peptide enhances PEG-mediated fusion only of highly curved, fusogenic vesicles at low P/L ratios but inhibits fusion at high P/L**. The requirement for high curvature is demonstrated by the fact that HA fusion peptide did not induce fusion of uncurved, nonfusogenic vesicles in the presence or absence of PEG (Figure 6). The observed effects of fusion peptide on PEG-mediated fusion of perturbed POPC LUV, which are uncurved but fusogenic vesicles, support this conclusion. Thus, Figure 7 shows that PEG-mediated fusion (contents mixing and lipid mixing) of these vesicles was *inhibited* and leakage was enhanced with increasing P/L ratio. Even fusion of highly curved SUVs, which was enhanced at low P/L (Figure 5) and depends on the surface tension of curved outer leaflets (*25*), is actually inhibited by high concentrations of fusion peptide (Figure 5). A possible interpretation of these results is that the HA fusion peptide fills the packing defects in SUV or perturbed LUV outer leaflets and inhibits the initial step of fusion (*47*).

This conclusion agrees with some reports in the literature. Rafalski et al. (*13*) reported contents leakage but not contents mixing between POPC LUV treated with the X-31 strain of HA fusion peptide. In addition, the synthetic peptide GALA, which was designed to mimic fusion peptide, has been reported to induce aggregation and leakage but not fusion of egg PC LUVs (*48*). In agreement with our conclusion about the importance of curvature, GALA did induce aggregation and perhaps fusion of POPC SUVs (whatever occurred was accompanied by very high leakage) (*49*). Finally, as for the HA fusion peptide, several articles have reported aggregation and lipid mixing between model membranes induced by the HIV fusion peptide. However, Nieva et al. (*50*) reported that HIVarg fusion peptide did not induce fusion of acidic-lipid LUVs unless Ca^{2+} was present, purportedly to alter the peptide conformation but possibly to induce vesicle aggregation, which we do with PEG.

(3) **Fusion peptide affects both the initial and subsequent steps of the fusion process, but it is unclear from the present study which is most affected**. PEG-mediated vesicle fusion (*47*) and probably HA-mediated fusion (*51*) proceed via a three-step process: outer-leaflet merger to create an initial reversible intermediate (stalk), conversion of this intermediate to an irreversible intermediate (transmembrane complex), and conversion of this intermediate to a fusion pore (fusion product). At low P/L, PEG-mediated lipid mixing and contents mixing for DOPC SUVs were both increased by fusion peptide, but at high P/L, lipid mixing persisted while contents mixing was inhibited (Figure 5). This suggests that the effect of fusion peptide in the initial and subsequent steps of fusion process may be different. The different effect of HA fusion peptide on lipid mixing and contents mixing can also be seen directly in Figure 5A. In the presence of 20 wt % PEG, contents mixing between DOPC SUVs was enhanced by roughly 85% (Figure 5A) while lipid mixing was increased by only about 20% (Figure 5C) due to the presence of fusion peptide at P/L = 0.004. This suggests that it is one of the two steps following formation of the initial intermediate that is most affected by fusion peptide. While the fusion peptide incorporates into the target membrane early in the fusion process (*52*), it may also incorporate into the viral membrane at some point during the fusion event (*8*). Schoch and Blumenthal (*53*) suggest that the fusion peptide plays an important role in later stages of the fusion process (pore widening). Our results suggest that it is either the step of final intermediate formation or the step of pore formation that is most affected by fusion peptide, although additional kinetic data will be needed to strengthen this conclusion.

What Is the Mechanism by Which HA Fusion Peptide Enhances PEG-Mediated Fusion? While our data do not directly address this point, it may be worthwhile to comment on it, given what is known about the effect of fusion peptide on bilayer structure. As mentioned earlier, PEG is known to lower the activity of water and thereby cause membrane dehydration leading to vesicles aggregation (*16*). PEG added externally to vesicles also creates an osmotic gradient leading to compressive lipid bilayer strain that can favor fusion, presumably through helping to stabilize areas of acyl chain packing mismatch associated with nonlamellar fusion intermediates (V. Malinin, unpublished observations). It is well-known that several viral fusion peptides disrupt bilayers at high peptide concentrations, as confirmed by our observations. This may reflect reports that the amino-terminal region of HA2 disrupts stable bilayer packing and induces negative curvature strain that favors inverted hexagonal phase structures (*54*). However, these reports of bilayer-disrupting ability of fusion peptide reflect effects seen at very high P/L ratios. At low peptide concentrations (<P/L = 0.005), bilayer surface properties remain unaltered by HA fusion peptide (Haque and Lentz, unpublished observations). Our guess at this point is that fusion peptide at low surface concentrations might enhance fusion in the same way that PEG-induced osmotic compression does, by somehow reducing the packing mismatch in the hydrophobic regions of the nonlamellar intermediate structures thought to be involved in the fusion process (*55*). In this way, PEG and fusion peptide might act synergistically to promote fusion of fusogenic membrane vesicles, as implied by our results.

REFERENCES

1. White, J., Kielian, M., and Helenius, A. (1983) *Q. Rev. Biophys. 16*, 151−95.
2. Hernandez, L. D., Peters, R. J., Delos, S. E., Young, J. A., Agard, D. A., and White, J. M. (1997) *J. Cell. Biol. 139*, 1455−64.
3. Chen, J., Lee, K. H., Steinhauer, D. A., Stevens, D. J., Skehel, J. J., and Wiley, D. C. (1998) *Cell 95*, 409−17.
4. Gething, M. J., Doms, R. W., York, D., and White, J. (1986) *J. Cell Biol. 102*, 11−23.
5. Skehel, J. J., Bayley, P. M., Brown, E. B., Martin, S. R., Waterfield, M. D., White, J. M., Wilson, I. A., and Wiley, D. C. (1982) *Proc. Natl. Acad. Sci. U.S.A. 79*, 968−72.

6. Carr, C. M., Chaudhry, C., and Kim, P. S. (1997) *Proc. Natl. Acad. Sci. U.S.A. 94*, 14306−13.
7. White, J. M. (1992) *Science 258*, 917−24.
8. Tsurudome, M., Gluck, R., Graf, R., Falchetto, R., Schaller, U., and Brunner, J. (1992) *J. Biol. Chem. 267*, 20225−32.
9. Pecheur, E. I., Sainte-Marie, J., Bienvenue, E. A., and Hoekstra, D. (1999) *J. Membr. Biol. 167*, 1−17.
10. Wharton, S. A., Martin, S. R., Ruigrok, R. W., Skehel, J. J., and Wiley, D. C. (1988) *J. Gen. Virol. 69*, 1847−57.
11. Lear, J. D., and DeGrado, W. F. (1987) *J. Biol. Chem. 262*, 6500−5.
12. Murata, M., Sugahara, Y., Takahashi, S., and Ohnishi, S. (1987) *J. Biochem. (Tokyo) 102*, 957−62.
13. Rafalski, M., Ortiz, A., Rockwell, A., van Ginkel, L. C., Lear, J. D., DeGrado, W. F., and Wilschut, J. (1991) *Biochemistry 30*, 10211−20.
14. Bailey, A. L., Monck, M. A., and Cullis, P. R. (1997) *Biochim. Biophys. Acta 1324*, 232−44.
15. Matsumoto, T. (1999) *Biophys. Chem. 79*, 153−62.
16. Lentz, B. R. (1994) *Chem. Phys. Lipids 73*, 91−106.
17. Mayer, L. D., Hope, M. J., and Cullis, P. R. (1986) *Biochim. Biophys. Acta 858*, 161−8.
18. Lentz, B. R., McIntyre, G. F., Parks, D. J., Yates, J. C., and Massenburg, D. (1992) *Biochemistry 31*, 2643−53.
19. Lentz, B. R., Carpenter, T. J., and Alford, D. R. (1987) *Biochemistry 26*, 5389−97.
20. Burack, W. R., Gadd, M. E., and Biltonen, R. L. (1995) *Biochemistry 34*, 14819−28.
21. Lee, J., and Lentz, B. R. (1997) *Biochemistry 36*, 421−31.
22. Mohandas, N., Wyatt, J., Mel, S. F., Rossi, M. E., and Shohet, S. B. (1982) *J. Biol. Chem. 257*, 6537−43.
23. Wu, H., Zheng, L., and Lentz, B. R. (1996) *Biochemistry 35*, 12602−11.
24. Ellens, H., Bentz, J., and Szoka, F. C. (1984) *Biochemistry 23*, 1532−8.
25. Talbot, W. A., Zheng, L. X., and Lentz, B. R. (1997) *Biochemistry 36*, 5827−36.
26. Burgess, S. W., and Lentz, B. R. (1993) *Methods Enzymol. 220*, 42−50.
27. Lentz, B. R., and Burgess, S. W. (1989) *Biophys. J. 56*, 723−33.
28. Koppaka, V., and Lentz, B. R. (1996) *Biophys. J. 70*, 2930−7.
29. Burgess, S. W., McIntosh, T. J., and Lentz, B. R. (1992) *Biochemistry 31*, 2653−61.
30. Massenburg, D., and Lentz, B. R. (1993) *Biochemistry 32*, 9172−80.
31. Lentz, B. R., Talbot, W., Lee, J., and Zheng, L. X. (1997) *Biochemistry 36*, 2076−83.
32. Epand, R. F., Martin, I., Ruysschaert, J. M., and Epand, R. M. (1994) *Biochem. Biophys. Res. Commun. 205*, 1938−43.
33. Chernomordik, L., Kozlov, M. M., and Zimmerberg, J. (1995) *J. Membr. Biol. 146*, 1−14.
34. White, J. M. (1990) *Annu. Rev. Physiol. 52*, 675−97.
35. Sarkar, D. P., Morris, S. J., Eidelman, O., Zimmerberg, J., and Blumenthal, R. (1989) *J. Cell Biol. 109*, 113−22.
36. Lowy, R. J., Sarkar, D. P., Chen, Y., and Blumenthal, R. (1990) *Proc. Natl. Acad. Sci. U.S.A. 87*, 1850−4.
37. Wiley, D. C., and Skehel, J. J. (1987) *Annu. Rev. Biochem. 56*, 365−94.
38. Carr, C. M., and Kim, P. S. (1993) *Cell 73*, 823−32.
39. Epand, R. F., Macosko, J. C., Russell, C. J., Shin, Y. K., and Epand, R. M. (1999) *J. Mol. Biol. 286*, 489−503.
40. Huang, R. T., Rott, R., and Klenk, H. D. (1981) *Virology 110*, 243−7.
41. Matlin, K. S., Reggio, H., Helenius, A., and Simons, K. (1981) *J. Cell Biol. 91*, 601−13.
42. Stegmann, T., Bartoldus, I., and Zumbrunn, J. (1995) *Biochemistry 34*, 1825−32.
43. Melikyan, G. B., and Chernomordik, L. V. (1997) *Trends Microbiol. 5*, 349−55.
44. Markosyan, R. M., Melikyan, G. B., and Cohen, F. S. (1999) *Biophys. J. 77*, 943−52.
45. Leikina, E., Markovic, I., Chernomordik, L. V., and Kozlov, M. M. (2000) *Biophys. J. 79*, 1415−1427.
46. Chanturiya, A., Leikina, E., Zimmerberg, J., and Chernomordik, L. V. (1999) *Biophys. J. 77*, 2035−45.
47. Lee, J., and Lentz, B. R. (1997) *Biochemistry 36*, 6251−9.
48. Parente, R. A., Nir, S., and Szoka, F. C., Jr. (1990) *Biochemistry 29*, 8720−8.
49. Parente, R. A., Nir, S., and Szoka, F. C., Jr. (1988) *J. Biol. Chem. 263*, 4724−30.
50. Nieva, J. L., Nir, S., Muga, A., Goni, F. M., and Wilschut, J. (1994) *Biochemistry 33*, 3201−9.
51. Lee, J., and Lentz, B. R. (1998) *Proc. Natl. Acad. Sci. U.S.A. 95*, 9274−9.
52. Harter, C., James, P., Bachi, T., Semenza, G., and Brunner, J. (1989) *J. Biol. Chem. 264*, 6459−64.
53. Schoch, C., and Blumenthal, R. (1993) *J. Biol. Chem. 268*, 9267−74.
54. Epand, R. M., and Epand, R. F. (1994) *Biochem. Biophys. Res. Commun. 202*, 1420−5.
55. Lentz, B. R., Malinin, V., Haque, M. E., and Evans, K. (2000) *Curr. Opin. Struct. Biol. 10*, 607−15.

BI011308L